Catalysis Today 141 (2009) 138–143

Contents lists available at ScienceDirect

Catalysis Today

journal homepage: www.elsevier.com/locate/cattod

Enhanced activity of methanol electro-oxidation on Pt–V_2O_5/C catalysts

P. Justin, G. Ranga Rao *

Department of Chemistry, Indian Institute of Technology Madras, Chennai 600036, India

ARTICLE INFO

Article history:
Available online 12 May 2008

Keywords:
Methanol oxidation
Pt–V_2O_5/C
Polyol method
Alkaline fuel cell
CO-TPD

ABSTRACT

The Vulcan carbon-supported vanadium oxide (V_2O_5) was prepared by solid-state reaction under intermittent microwave heating (IMH) method. Pt nanoparticles were dispersed by microwave-assisted polyol process over Vulcan carbon and V_2O_5/C. The catalyst samples were characterized by PXRD, TEM, CO-TPD and electrochemical methods. The TEM images showed homogeneous dispersion of ~3 nm size Pt metal crystallites embedded over Vulcan carbon support. The activities of Pt/C and Pt–V_2O_5/C for electrochemical oxidation of methanol were studied in 1.0 M KOH solution by cyclic voltammetry, chronoamperometry and chronopotentiometry. The influence of V_2O_5 component on the activity of Pt–V_2O_5/C was screened for catalytic oxidation of methanol. The results show that Pt–V_2O_5(4:3)/C composite catalyst performed better than Pt/C catalyst for methanol oxidation. The temperature programmed desorption (TPD) with CO was carried out to assess the CO tolerance of Pt–V_2O_5/C electrocatalyst. The formation of oxygen-containing species at lower potential can transform CO-like poisoning species on Pt to CO_2 in the presence of V_2O_5 which helps in regenerating active sites on Pt for further electrochemical oxidation of methanol. The enhanced electrode response is attributed to synergistic effect between Pt and V_2O_5.

1. Introduction

Direct methanol fuel cells (DMFCs) have been documented as promising power sources for compact, high-power density energy conversion [1,2]. Methanol has low-theoretical oxidation potential (E° = 0.03 V) comparable to that of hydrogen (E° = 0 V). Methanol is considered as an efficient fuel which can be obtained from natural gas, coal and biomass. It is an excellent energy carrier in the form of liquid at room temperature and atmospheric pressure. Unlike hydrogen, storage and utilization of liquid methanol does not need extensive modification of the existing fuel infrastructure. Despite these advantages, high over potentials for methanol oxidation and methanol crossover from anode to cathode through membrane prevent the use of DMFCs in practical applications. The strong adsorption of carbon monoxide on Pt anode inhibits the methanol oxidation reaction [3]. The electrocatalytic activities of anode are significantly enhanced when Pt is alloyed with Ru, Os, Ir, Rh, Mo and Sn either by modifying the electronic properties of Pt or by modifying the surface chemistry in which bifunctional reaction mechanism has been invoked to promote the oxidation of CO to CO_2 [4–10]. The multicomponent catalysts have exhibited superior performance relative to Pt metal, and so far, the incorporation of Ru into the Pt catalyst has yielded the best results. However, there is a need to reduce the loading of expensive noble metals and also improve the susceptibility of bimetallic electrocatalyst towards CO poisoning [11,12].

The anodic oxidation of methanol in alkaline media is more feasible than in acidic media. The open circuit potential of oxygen reduction is more positive in alkaline media than in acidic media [13]. In addition, the CO poisoning of the Pt catalyst is less likely in alkaline solution than in acidic solution. However, the problem with alkaline media is the progressive carbonation of solution due to CO_2 from air or the oxidation product of the fuel. The progressive carbonation of alkaline media has been addressed by the application of alkaline anion exchange membranes (AAEM) [14–16] and/or fuel-flexible, media-flexible laminar flow fuel cells [17,18]. Recently, Pt promoted oxides such as CeO_2 [19], ZrO_2 [20] and MgO [21] have been used as electrocatalysts for direct oxidation of alcohol in alkaline medium which significantly improved the electrode performance by enhanced activity and poison resistance. Although recent reports have demonstrated that Pt-based catalysts have higher activity for methanol oxidation, both in alkaline and acidic media, there is scope to reduce the catalyst loading for economic viability.

The supported vanadium oxides find catalytic applications in oxidative dehydrogenation (ODH) of propane [22] and selective catalytic reduction of NO_x by ammonia [23]. The vanadium-modified Pt catalysts have been applied for diesel engine exhaust gas conversion [24], and oxidation of organic compounds [25]. Various morphologies of vanadium oxide (V_2O_5) in the nano-regime

* Corresponding author. Tel.: +91 44 2257 4226; fax: +91 44 2257 4202.
E-mail address: grrao@iitm.ac.in (G.R. Rao).

0920-5861/$ – see front matter © 2008 Elsevier B.V. All rights reserved.
doi:10.1016/j.cattod.2008.03.019

have been synthesized and their utility as electrode materials is tested for lithium-ion batteries [26], electrochemical capacitors [27] and electrochemical sensors [28]. Surnev et al. have recently reviewed the surface and structural chemistry of vanadium oxide nano-layers in the context of catalysis [29]. Vanadium oxide layers exhibit redox and Lewis acid/base properties which are important for catalyzing surface reactions. In this communication we present the results on V_2O_5 incorporated Pt/C catalysts for direct electrochemical oxidation of methanol in alkaline solutions. A systematic electrochemical characterization of Pt–V_2O_5/C electrocatalysts for methanol oxidation is reported in this paper. The specific issues related to the CO tolerance of Pt metal-based fuel cell catalysts, the optimum Pt metal/V_2O_5 ratio, the possibility of improving catalytic activity, and the utilization of Pt metal are presented in this paper.

2. Experimental

2.1. Preparation of Pt/C or Pt–V_2O_5/C electrocatalysts

The V_2O_5/C used in this study was prepared by a solid-state reaction under intermittent microwave heating (IMH) method. In brief, the V_2O_5 (99.9% purity, Thomas Baker, India) powder was well dispersed over Vulcan XC-72R carbon (Cabot Corp., USA) using 2-propanol as solvent and the mixture was dried in oven at 80 °C. The mixture was then introduced into a microwave oven (Sharp NN-S327 WF, 2450 MHz, 1100 W) and heated six times, each time for 20 s followed by a 60 s pause. The Pt nanoparticles are supported over Vulcan carbon or V_2O_5/C by microwave-assisted polyol process [30]. Typically 1.0 ml of 0.05 M $H_2PtCl_6{\cdot}6H_2O$ (Aldrich, A.C.S. Reagent) was mixed with 25 ml of ethylene glycol (AR grade) in 100 ml beaker. 0.4 M KOH (in ethylene glycol) was added drop wise to adjust the pH of the solution to about 10 in order to induce the formation of small and uniform Pt nanoparticles. This mixture was sonicated after adding Vulcan carbon (in the case of Pt/C catalyst) or V_2O_5/C (in the case of Pt–V_2O_5/C catalyst) and the resulting mixture was subjected to microwave heating for 50 s. The sample under microwave irradiation was boiling at temperature approximately <300 °C since the boiling point of ethylene glycol is 197.3 °C. The resulting suspension was filtered and the residue was washed with acetone and dried at 25 °C in a vacuum oven overnight. The amount of V_2O_5 is varied at fixed amounts of Pt (0.01 g) and Vulcan carbon (0.04 g) in all four samples (Table 1).

2.2. Characterization of Pt/C and Pt–V_2O_5/C electrocatalysts

The reduction of Pt from their salts was monitored in the region of 200–800 nm by JASCO V 530 UV–vis spectrophotometer employing 1 cm path length quartz cuvettes. The phases and lattice parameters of catalyst samples were characterized by powder X-ray diffraction (PXRD) patterns employing Shimadzu XD-D1 diffractometer using Cu Kα radiation (λ = 1.5418 Å) operating at 30 kV and 20 mA. The particle morphology, size, and size distribution of catalysts were characterized by JEOL JEM-3010 transmission electron microscopy (TEM) at 200 kV operating voltage. Temperature-programmed desorption of carbon monoxide measurements were carried out using Micromeritics Chemisorb 2750 instrument under He flow (10 cm^3/min) at atmospheric pressure. Prior to the experiment, catalyst samples were activated at 200 °C in 5% H_2 in Ar for 1 h. The sample was cooled to room temperature in the same atmosphere and flushed with pure He for 15 min before CO chemisorption was carried out at room temperature for 1 h using 10.85% CO in He. The CO desorption profiles were recorded from room temperature to 300 °C at a heating rate of 10 °C/min.

2.3. Electrochemical measurements

The working electrodes for electrochemical measurements were fabricated by dispersing Pt/C or Pt–V_2O_5/C powders in 1.0 ml of distilled water and 5 wt% Nafion (75 μL). Ultrasonic treatment was given for 15 min to achieve uniform dispersion of the mixture at room temperature. A known amount of suspension was deposited on the surface of a glassy carbon electrode and the solvent was slowly evaporated. Finally, a drop of 1.0 wt% Nafion in ethanol solution was covered on top to prevent damage of the catalyst layer. The Pt loadings on Pt/C and Pt–V_2O_5/C electrodes were normally controlled at 0.3 mg cm^{-2}. Electrochemical measurements were carried out in a conventional three-electrode cell by using CHI 660B electrochemical workstation. A platinum foil and 1.0 M KOH|Hg/HgO (CHI Instruments, USA) were used as counter and reference electrodes, respectively. The test solution consists of 1 M CH_3OH and 1 M KOH. The dissolved oxygen was removed by purging the solution with pure nitrogen for 30 min before starting the electrochemical experiment.

3. Results and discussion

3.1. Physicochemical characterization of Pt/C and Pt–V_2O_5/C catalysts

The formation of Pt nanoparticles using microwave dielectric heating has been monitored by UV–vis spectroscopy. The H_2PtCl_6 solution before microwave irradiation is pale yellow and shows an absorption band at 264 nm due to ligand-to-metal charge-transfer transition in $PtCl_6^{2-}$ ion [31]. The pale-yellow color solution has become colorless after completion of the reaction. The disappearance of the band at 264 nm is verified suggesting complete reduction of $PtCl_6^{2-}$ ions (Eq. (1)):

$$PtCl_6^{2-} + CH_2OH - CH_2OH \rightarrow Pt^0 + CHO - CHO + 4H^+ + 6Cl^- \quad (1)$$

Table 1
Onset potentials and peak current densities obtained for the oxidation of methanol with different V_2O_5 loadings, and comparison of surface areas obtained from electrochemical and PXRD measurements

Catalyst	Onset potential (V)	i_p[a] (mA cm^{-2})	Q_H[b] (mC g^{-1} Pt)	EAS[c] (m^2 g^{-1} Pt)	S[d] (m^2 g^{-1} Pt)
Pt/C	−0.35	101	56.6	90 ± 10	107 ± 12
Pt–V_2O_5(4:1)/C	−0.35	121	–	–	–
Pt–V_2O_5(2:1)/C	−0.39	179	–	–	–
Pt–V_2O_5(4:3)/C	−0.42	200	59.8	94 ± 10	111 ± 12
Pt–V_2O_5(1:1)/C	−0.37	110	–	–	–

[a] Peak current density from cyclic voltammetry.
[b] Charge exchanged during the electroadsorption of hydrogen atoms on Pt particles.
[c] Surface area of Pt particles from electrochemical measurement.
[d] Surface area of Pt crystallites obtained from PXRD.

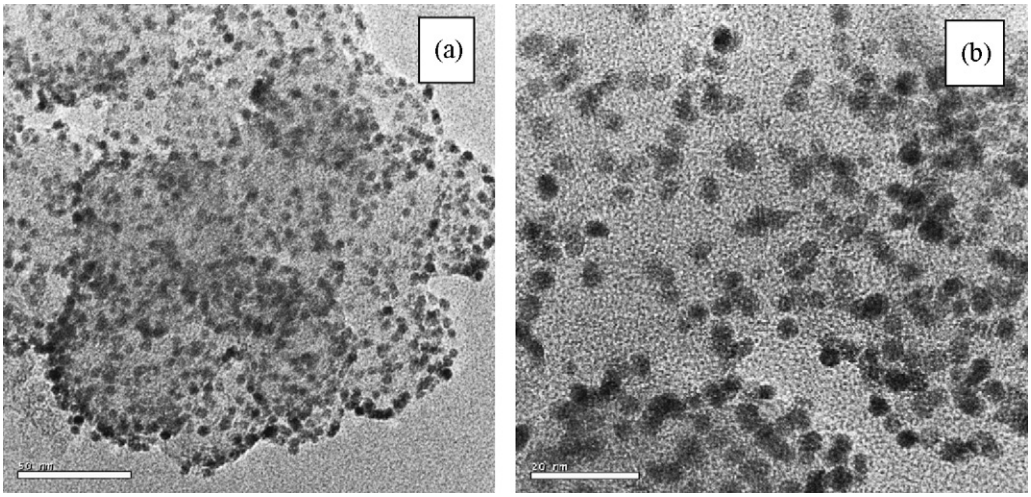

Fig. 1. TEM micrographs of the Pt–V_2O_5(4:3)/C electrocatalyst: (a) 50 nm scale and (b) 20 nm scale.

The high dielectric constant (41.4 at 298 K) and the dielectric loss of ethylene glycol speed up heating process under microwave irradiation. Here ethylene glycol also acts as a reducing agent producing metal particle from metal ions. Rapid heating by microwave accelerates the reduction of metal precursor and the nucleation of metal particles. Homogeneous microwave heating of liquid samples has an advantage of reducing the temperature and concentration gradients in the reaction medium and providing uniform environment for nucleation and growth of metal nanoparticles.

The transmission electron microscope (TEM) image of Pt–V_2O_5/C electrocatalyst is shown in Fig. 1. Homogeneous dispersion of small and uniformly dispersed spherical Pt metal particles (dark spots) with size of about 2–3 nm embedded in V_2O_5/C support are seen in the TEM images. This is further confirmed by average crystallite size analysis from (2 2 0) diffraction peak of Pt fcc lattice by Scherrer equation. The estimated surface area values are given in Table 1.

The powder XRD patterns of as-synthesized Pt/C and Pt–V_2O_5/C catalysts are given in Fig. 2. The broad diffraction peak observed at 24.5° is due to the (0 0 2) reflection of hexagonal Vulcan carbon. The peaks at $2\theta = 40.1°$ (1 1 1), 46.6° (2 0 0) and 68.1° (2 2 0) reflections can be indexed to Pt crystallites in the catalyst samples. The diffraction peak at $2\theta = 40.1°$ for Pt(1 1 1) corresponds to the inter-planar spacing of $d_{1\,1\,1} = 0.224$ nm and a lattice constant of 0.389 nm. The diffraction patterns of the prepared catalyst agree well with standard powder diffraction patterns of Pt (JCPDS 1-1311). The mean crystallite size calculated from the isolated Pt(2 2 0) peak is ~3.1 nm for Pt/C and ~2.6 nm for Pt–V_2O_5/C catalyst samples. The Pt particles in V_2O_5-modified catalysts are smaller in size compared to Pt particles synthesized on carbon support alone. Thus ethylene glycol reduction method is suitable to produce nano-range uniform size Pt nanoparticles for electrocatalytic applications. The PXRD pattern of V_2O_5-modified Pt catalysts do not show the reflections related to V_2O_5 phase. But the diffraction peaks of Pt–V_2O_5/C are slightly shifted to lower values when compared to Pt/C. This is an indication that an alloy between Pt and V_2O_5 is being formed on the Pt–V_2O_5/C catalysts. The alloying of Pt–V is possible due to the Tammann temperature ($T_{Tam} = T_{mp}/2$) of V_2O_5 at 209 °C where the surface vanadium ions begin to diffuse and react with Pt particles [32]. There is a specific interaction between vanadium oxide layers and Pt particles leading to interfacial alloy formation in the electrocatalytic material which may be critical in enhancing the catalytic activity for methanol oxidation. Interfacial vanadium oxide layers and crystallites are often elusive to powder XRD and known to show reactivity higher than the bulk oxide [29].

The CO-TPD experiment has been carried to evaluate the resistance of catalyst surface poisoning by CO and its possible affect on the activity of electro-oxidation of methanol [33]. The CO-TPD profiles of Pt–V_2O_5/C electrocatalyst in comparison with that of Pt/C and V_2O_5 are shown in Fig. 3. The CO desorption is observed from Pt/C catalyst as broad peaks below 100 °C and above 200 °C. A maximum CO desorption rate from Pt/C electrocatalyst is located at 62 °C in the low-temperature region due to physisorbed CO. The CO desorption from pure platinum occurs above 187 °C [34]

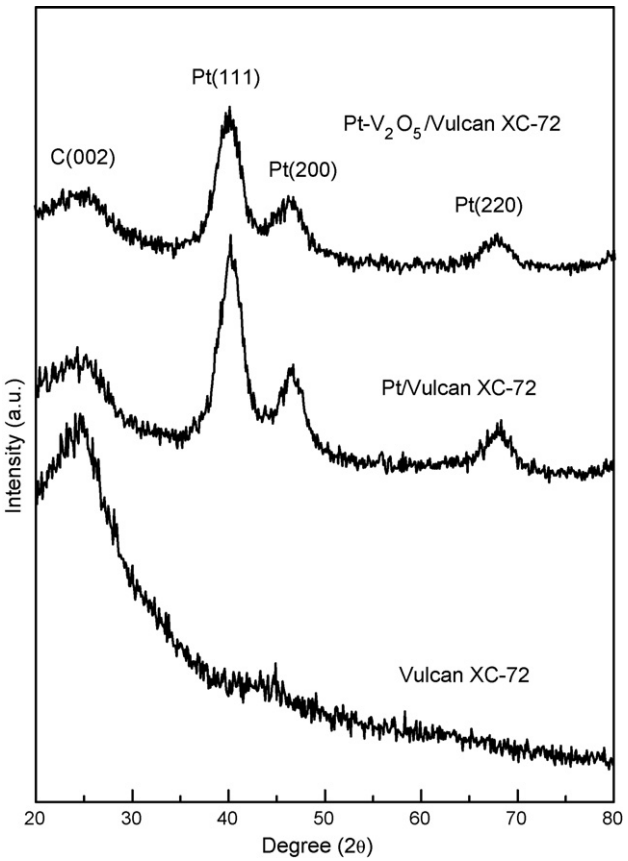

Fig. 2. PXRD spectra of Vulcan XC-72, Pt/Vulcan XC-72 and Pt–V_2O_5(4:3)/Vulcan XC-72 catalysts.

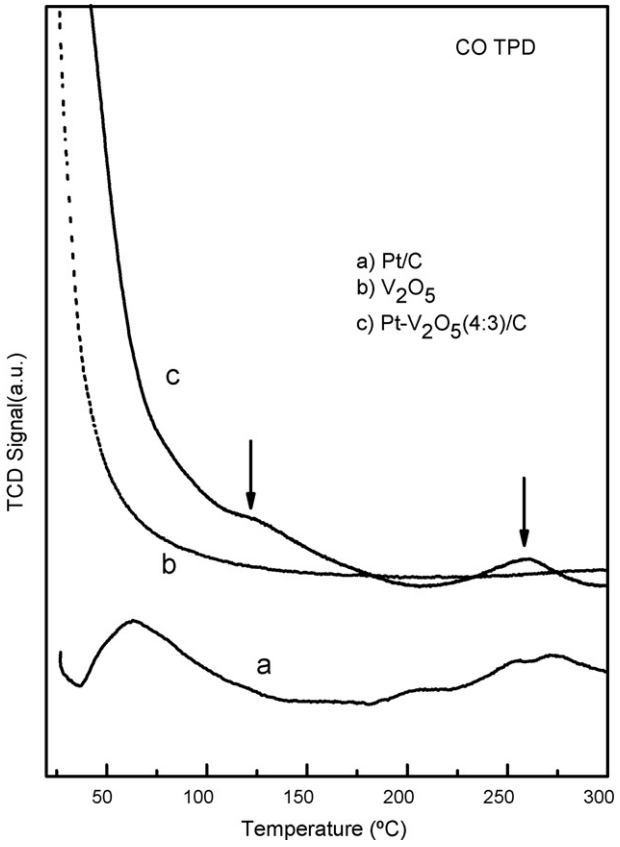

Fig. 3. CO-TPD profiles of Pt/C, V_2O_5 and Pt–V_2O_5(4:3)/C catalysts.

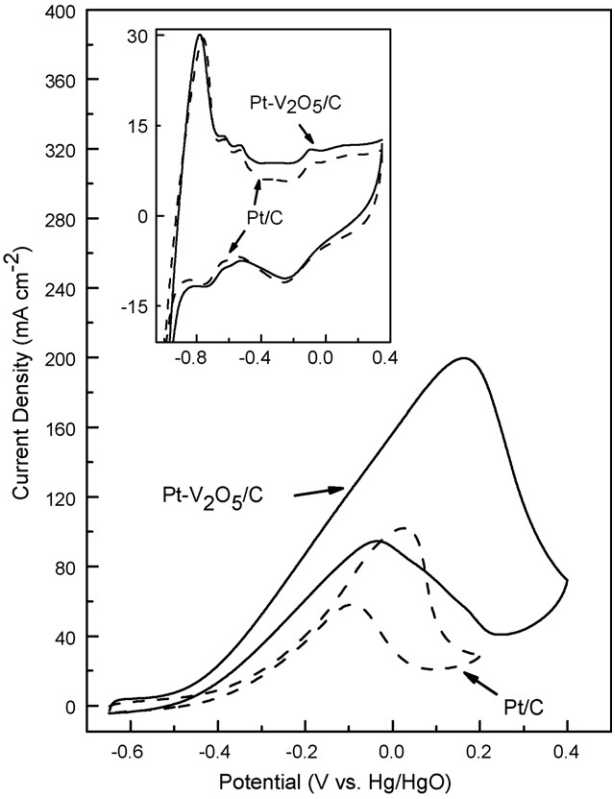

Fig. 4. Cyclic voltammograms for electro-oxidation of methanol on Pt/C and Pt–V_2O_5(4:3)/C electrodes in 1.0 mol dm^{-3} KOH + 1.0 mol dm^{-3} CH_3OH. Inset shows the hydrogen electroadsorption voltammetric profiles of Pt/C and Pt–V_2O_5(4:3)/C electrodes in 1.0 mol dm^{-3} KOH. All the voltammograms are recorded using 50 mV s^{-1} scan rate and 0.3 mg cm^{-2} Pt loading at room temperature.

whereas from defective V_2O_5 at 127 °C [35]. Under the experimental conditions employed, no CO or CO_2 desorption is observed on V_2O_5, except the ambient and/or physisorbed CO feature below 50 °C (Fig. 3(b)). In sharp contrast, Pt–V_2O_5/C catalysts exhibit significantly different desorption profile with CO peaks at 120 and 260 °C. The peak at 120 °C corresponds to the CO adsorbed on defect sites at metal oxide interface while the peak at 260 °C is result of the CO adsorbed on Pt particles [34]. The defect sites are known to stabilize a variety of adsorbed CO species at the metal-oxide interfaces, and CO molecules adsorbed on metallic sites tend to spill-over to the interfacial sites [36]. Therefore, the V_2O_5 component in the Pt–V_2O_5/C catalysts may play an important role of scavenging the adsorbed CO on Pt particles. There is a possibility that V_2O_5 oxide surface can facilitate the conversion of adsorbed CO to CO_2. The removal of adsorbed CO from Pt particles at lower temperatures reduces the poisoning effect on catalyst surface. This in turn can have an enhanced effect on the electrocatalytic activity of Pt–V_2O_5/C for electro-oxidation of methanol.

3.2. Electrochemical characterization of Pt/C and Pt–V_2O_5/C catalysts

The electrochemical active surface area (EAS) of Pt catalyst is usually determined by hydrogen underpotential deposition (H-UPD) method as shown in the inset of Fig. 4. This method is based on the fact that each surface atom of Pt adsorbs one hydrogen atom. The charge associated with adsorption–desorption reactions provides the number of active Pt sites and the electrochemical active surface area. The EAS (m^2 g^{-1}) is calculated according to Eq. (2) [37]:

$$\text{EAS}\,(\text{m}^2\,\text{g}^{-1}\,\text{Pt}) = \frac{Q_H}{[\text{Pt}]0.21\,(\text{mC}\,\text{g}^{-1}\,\text{Pt})} \quad (2)$$

where [Pt] represents the platinum loading (mg cm^{-2}) in the electrode and Q_H represents the mean value between the amounts of charge exchanged during hydrogen adsorption–desorption peaks after subtracting the contribution from the double layer region (mC cm^{-2}). The value 0.21 represents the charge in mC cm^{-2} required to oxidize a monolayer of H_2 on polycrystalline Pt electrodes which is calculated from the surface density of 1.3×10^{15} atom cm^{-2}. The EAS for Pt/C and Pt–V_2O_5/C catalysts are determined from the inset of Fig. 4 as 90 and 94 m^2 g^{-1}, respectively. The results show that the electrochemical active surface area values are similar for both the electrodes. Despite similar EAS values, the Pt–V_2O_5/C electrode shows higher activity than Pt/C electrode for methanol electrochemical oxidation. Therefore the enhancement of electrochemical activity of Pt–V_2O_5/C is essentially due to the contribution of vanadia component effectively oxidizing the adsorbed CO to CO_2. This process helps regenerating the active sites for further oxidation of methanol. The specific surface area S (m^2 g^{-1}) of Pt particles has been calculated using Eq. (3) [38] and the results are summarized in Table 1:

$$S\,(\text{m}^2\,\text{g}^{-1}\,\text{Pt}) = \frac{6000}{\rho d} \quad (3)$$

where d is the mean crystallite size in nm calculated from Scherrer formula and ρ is the density of platinum metal (21.4 g cm^{-3}). The data are in good agreement with the electrochemical active surface area obtained by electrochemical method (Table 1).

Fig. 4 shows the cyclic voltammograms for methanol electro-oxidization over Pt/C and Pt–V_2O_5/C electrocatalysts in 1.0 M CH_3OH/1.0 M KOH electrolyte at room temperature. The observed

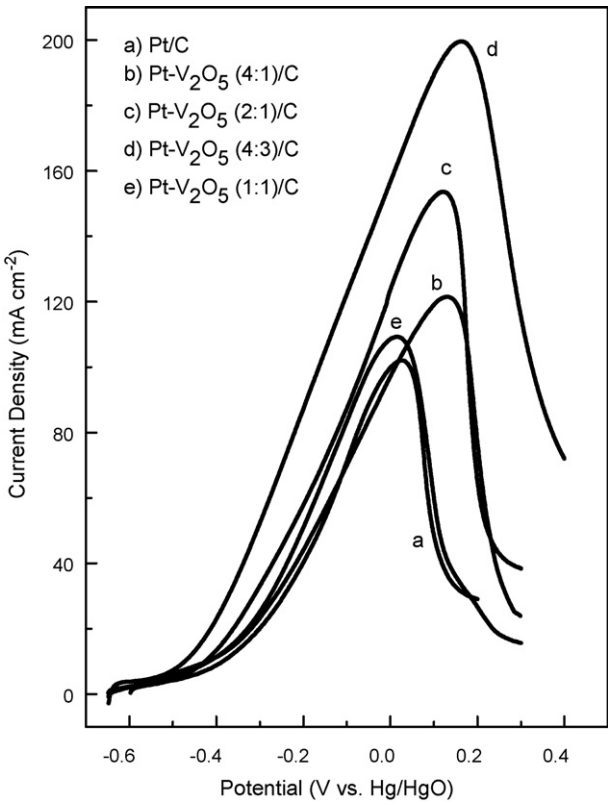

Fig. 5. Cyclic voltammograms for electro-oxidation of methanol on Pt/C and Pt–V_2O_5/C electrodes with varying amounts of V_2O_5 in 1.0 mol dm^{-3} KOH + 1.0 mol dm^{-3} CH_3OH solutions at room temperature. For clarity only forward scans are shown here. Scan rate = 50 mV s^{-1}; Pt loading = 0.3 mg cm^{-2}.

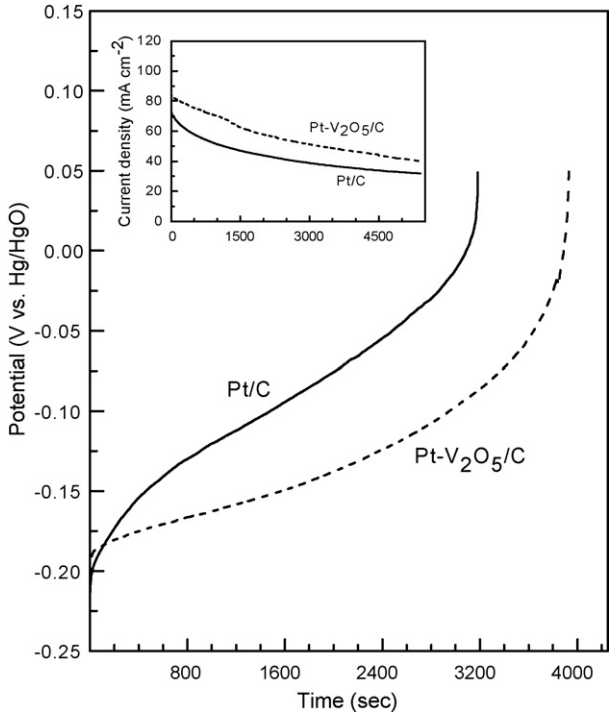

Fig. 6. Chronopotentiometric curves of methanol oxidation on Pt/C and Pt–V_2O_5(4:3)/C electrodes at 5 mA cm^{-2}. Inset shows the chronoamperometry curves of methanol oxidation on Pt/C and Pt–V_2O_5(4:3)/C electrodes at 0.1 V with respect to Hg/HgO. Both experiments are done in 1.0 mol dm^{-3} KOH + 1.0 mol dm^{-3} CH_3OH solutions at room temperature with 0.3 mg cm^{-2} Pt loading.

onset potentials for methanol oxidation are about −0.39 V for Pt/C and −0.49 V for Pt–V_2O_5/C with respect to Hg/HgO reference electrode. The peak current densities for Pt/C and Pt–V_2O_5/C catalysts are about 102 and 200 mA cm^{-2}, respectively, at a scan rate of 50 mV s^{-1}. Both the electrocatalysts show large methanol oxidation currents between −0.1 and 0.2 V with respect to Hg/HgO reference electrode. The Pt–V_2O_5/C catalyst exhibited nearly twofold increment in peak current density relative to Pt/C. The onset potentials shift to more negative direction for Pt–V_2O_5/C electrode relative to Pt/C electrode indicating that the former is more active for methanol oxidation. The twofold increment in methanol oxidation activity of Pt–V_2O_5/C electrode is attributed to faster removal of CO and facilitating methanol adsorption on fresh and regenerated Pt sites in the presence of V_2O_5. Therefore using the same amount of Pt, we could generate higher electrocatalytic currents in the case of Pt–V_2O_5/C electrode. This approach has been reported to be successful in the case of CeO_2 [19], ZrO_2 [20] and MgO [21]. Furthermore, the catalytic current of Pt–V_2O_5/C electrode begins to rise sharply at more negative potential which can contribute substantially to the overall cell efficiency.

The amount of V_2O_5 in Pt–V_2O_5/C catalysts too has a significant role to play in the electrocatalytic activity for methanol oxidation. The optimum weight ratio of Pt/V_2O_5 has been identified by changing the weight ratios of Pt and V_2O_5 at fixed platinum loading. Cyclic voltammetry studies have been performed to determine the effect of various ratios of Pt/V_2O_5 on methanol oxidation by fixing platinum loading to 0.30 mg cm^{-2}. It is seen in Fig. 5 that the peak current density increases with V_2O_5 content and at the same time the onset potential is shifted more towards negative side. The best performance is found when V_2O_5 loading is about 0.225 mg cm^{-2}, or the weight ratio of Pt and V_2O_5 is 4:3. Further increase in V_2O_5 oxide content diminishes the electrode conductivity and also affects its performance due to the inhibition of methanol adsorption on Pt sites.

The changes in voltage with time recorded for both the catalysts at a bias current of 5 mA cm^{-2} employing chronopotentiometric method are illustrated in Fig. 6. The potential increases with polarization time and finally shifts to a higher potential for oxygen evolution indicating the poisoning of the catalysts. The rapid increase in over potential is due to the formation of intermediate products of methanol oxidation such as CO and other ions in the electrolyte. The intermediate products are easily adsorbed on Pt surface and inhibit further methanol electro-oxidation. The polarization potentials are relatively lower for Pt–V_2O_5(4:3)/C electrocatalysts because the catalyst can withstand against poisoning species for longer time. The Pt–V_2O_5(4:3)/C electrocatalysts unequivocally exhibit better performance in comparison to Pt/C as a result of electrode poisoning-resistance in terms of reaction activity. The V_2O_5 component in the electrocatalyst seems to assist in generating oxygen-containing species at lower potential and convert CO-like poisoning species on Pt surface to CO_2. This observation is consistent with the CO-TPD result and the Pt–V_2O_5 interfacial region appears to be important for CO scavenging.

The time-dependent behavior of the Pt/C and Pt–V_2O_5(4:3)/C electrocatalysts toward methanol oxidation have been studied by chronoamperometry. The chronoamperometry behavior of Pt/C and Pt–V_2O_5/C electrocatalysts at the bias of 0.1 V with respect to Hg/HgO reference electrode in CH_3OH/1 M KOH electrolyte at room temperature for 5400 s are presented in the inset of Fig. 6. Both initial and limiting current densities of Pt–V_2O_5/C are higher than those obtained for Pt/C catalyst in the entire time range. The Pt–V_2O_5/C electrode shows higher electrochemical activity than Pt/C electrode for methanol oxidation at the bias potential of 0.1 V.

The behavior of Pt–V_2O_5/C sample is also consistent with the cyclic voltammograms shown in Fig. 4. Therefore, V_2O_5 is acting as a promoter when added to Pt/C electrode and helps improving the poison tolerance of the electrocatalyst.

4. Conclusions

The nanosized Pt/C and Pt–V_2O_5/C electrocatalytic materials prepared by microwave-assisted polyol process are tested for electrocatalytic properties. The Pt–V_2O_5/C catalyst shows higher catalytic activity towards methanol oxidation reaction compared to that of Pt/C. V_2O_5 acts as a promoter to Pt catalysts for enhancing the electrode performance by twofold for methanol oxidation. The higher activity and better poison resistance of the Pt–V_2O_5/C catalyst is attributed to the synergistic effect between Pt and V_2O_5 promoter.

Acknowledgment

The financial support by the Defence Research and Development Organization (DRDO), New Delhi (Grant no. ERIP/ER/0300231/M/01) is gratefully acknowledged.

References

[1] S. Wasmus, A. Kuver, J. Electroanal. Chem. 461 (1999) 14.
[2] G.J.K. Acres, J.C. Frost, G.A. Hards, R.J. Potter, T.R. Ralph, D. Thompsett, G.T. Burstein, G.J. Hutchings, Catal. Today 38 (1997) 393.
[3] K. Scott, W.M. Taama, P. Argyropoulos, K. Sundmacher, J. Power Sources 83 (1999) 204.
[4] T. Frelink, W. Visscher, J.A.R. van Veen, Langmuir 12 (1996) 3702.
[5] B. Beden, F. Kadirgan, C. Lamy, J.M. Leger, J. Electroanal. Chem. 127 (1981) 75.
[6] B. Gurau, R. Viswanathan, R.X. Liu, T.J. Lafrenz, K.L. Ley, E.S. Smotkin, E. Reddington, A. Sapienza, B.C. Chan, T.E. Mallouk, S. Sarangapani, J. Phys. Chem. B 102 (1998) 9997.
[7] A.S. Arico, V. Antonucci, N. Giordano, A.K. Shukla, M.K. Ravikumar, A. Roy, S.R. Barman, D.D. Sarma, J. Power Sources 50 (1994) 295.
[8] W. Chrzanowski, A. Wieckowski, Langmuir 14 (1998) 1967.
[9] A. Crown, I.R. Moraes, A. Wieckowski, J. Electroanal. Chem. 500 (2001) 333.
[10] S. Jayaraman, A.C. Hillier, J. Phys. Chem. B 107 (2003) 5221.
[11] J.S. Lee, K.I. Han, S.O. Park, H.N. Kim, H. Kim, Electrochim. Acta 50 (2004) 807.
[12] V. Raghuveer, B. Viswanathan, Fuel 81 (2002) 2191.
[13] R. Parsons, T. VanderNoot, J. Electroanal. Chem. 257 (1988) 9.
[14] K. Matsuoka, Y. Iriyama, T. Abe, M. Matsuoka, Z. Ogumi, J. Power Sources 150 (2005) 27.
[15] J.R. Varcoe, R.C.T. Slade, E.L.H. Yee, Chem. Commun. (2006) 1428.
[16] C.C. Yang, S.J. Chiu, W.C. Chien, J. Power Sources 162 (2006) 21.
[17] R.S. Jayashree, L. Gancs, E.R. Choban, A. Primak, D. Natarajan, L.J. Markoski, P.J.A. Kenis, J. Am. Chem. Soc. 127 (2005) 16758.
[18] M.H. Chang, F. Cheng, N.S. Fang, J. Power Sources 159 (2006) 810.
[19] C. Xu, P.K. Shen, Chem. Commun. (2004) 2238.
[20] Y. Bai, J. Wu, J. Xi, J. Wang, W. Zhu, L. Chen, X. Qiu, Electrochem. Commun. 7 (2005) 1087.
[21] C. Xu, P.K. Shen, X. Ji, R. Zeng, Y. Liu, Electrochem. Commun. 7 (2005) 1305.
[22] H. Fu, Z.P. Liu, Z.H. Li, W.N. Wang, K.N. Fan, J. Am. Chem. Soc. 128 (2006) 11114.
[23] A.F. Popa, P.H. Mutin, A. Vioux, G. Delahay, B. Coq, Chem. Commun. (2004) 2214.
[24] M. Tischer, L.T. Ger, H. Klein, R. Domesle, E.S. Lox, G. Prescher, K. Seibold, P. Albers, Phys. Chem. Chem. Phys. 1 (1999) 2815.
[25] E.N. Ndifor, T. Garcia, S.H. Taylor, Catal. Lett. 110 (2006) 125.
[26] G. Li, S. Pang, L. Jiang, Z. Guo, Z. Zhang, J. Phys. Chem. B 110 (2006) 9383.
[27] R.N. Reddy, R.G. Reddy, J. Power Sources 156 (2006) 700.
[28] C.J. Mao, H.C. Pan, X.C. Wu, J.J. Zhu, H.Y. Chen, J. Phys. Chem. B 110 (2006) 14709.
[29] S. Surnev, M.G. Ramsey, F.P. Netzer, Prog. Surf. Sci. 73 (2003) 117.
[30] W.X. Chen, J.Y. Lee, Z. Liu, Chem. Commun. (2002) 2588.
[31] Z. Zhou, S. Wang, W. Zhou, G. Wang, L. Jiang, W. Li, S. Song, J. Liu, G. Sun, Q. Xin, Chem. Commun. (2003) 394.
[32] I.E. Wachs, Y. Chen, J. Jehng, L.E. Briand, T. Tanaka, Catal. Today 78 (2003) 13.
[33] R. Ganesan, J.S. Lee, Angew. Chem. Int. Ed. 44 (2005) 6557.
[34] G. Ertl, M. Neumann, K.M. Streit, Surf. Sci. 64 (1977) 393.
[35] D.S. Toledano, V.E. Henrich, J. Vac. Sci. Technol. A 18 (2000) 1906.
[36] G. Ranga Rao, H. Kondoh, H. Nozoye, Surf. Sci. 336 (1995) 287.
[37] A. Pozio, M.D. Francesco, A. Cemmi, F. Cardellini, L. Giorgi, J. Power Sources 105 (2002) 13.
[38] G. Tamizhmani, J.P. Dodelet, D. Guayt, J. Electrochem. Soc. 143 (1996) 18.